Am J Cancer Res 2024;14(1):227-242
www.ajcr.us /ISSN:2156-6976/ajcr0154364

Brief Communication

High *EIF4EBP1* expression reflects mTOR pathway activity and cancer cell proliferation and is a biomarker for poor breast cancer prognosis

Erek D Nelson[1*], Matthew GK Benesch[1*], Rongrong Wu[1,2*], Takashi Ishikawa[2], Kazuaki Takabe[1,2,3,4,5,6]

[1]Department of Surgical Oncology, Roswell Park Comprehensive Cancer Center, Buffalo, NY 14263, USA; [2]Department of Breast Surgery and Oncology, Tokyo Medical University, Tokyo 160-8402, Japan; [3]Department of Gastroenterological Surgery, Yokohama City University Graduate School of Medicine, Yokohama 236-0004, Japan; [4]Division of Digestive and General Surgery, Niigata University Graduate School of Medical and Dental Sciences, Niigata 951-8520, Japan; [5]Department of Breast Surgery, Fukushima Medical University School of Medicine, Fukushima 960-1295, Japan; [6]Department of Surgery, University at Buffalo Jacobs School of Medicine and Biomedical Sciences, State University of New York, Buffalo, NY 14263, USA. [*]Equal contributors.

Received November 11, 2023; Accepted December 21, 2023; Epub January 15, 2024; Published January 30, 2024

Abstract: Eukaryotic translation initiation factor 4E binding protein 1 (EIF4EBP1) is regulated by the mTOR (mammalian target of rapamycin) signaling pathway. Phosphorylated EIF4EBP1 protein leads to pathway activation and correlates with aggressive breast cancer features. However, the clinical relevance of *EIF4EBP1* gene expression as a prognostic biomarker in bulk breast tumors is not understood. In this study, *EIF4EBP1* expression was analyzed in over 5000 breast cancers from three large independent cohorts, TCGA, METABRIC, and SCAN-B (GSE96058), and expression was dichotomized into low and high groups by the median. We also performed gene set enrichment analysis (GSEA) and cell cybersorting via the xCell algorithm to investigate *EIF4EBP1* biology and expression patterns within the tumor microenvironment (TME). We additionally confirmed *EIF4EBP1* expression location in the TME via single cell RNA sequencing. *EIF4EBP1* expression was highest in both triple negative and high-grade tumors (both P<0.001), and tumor mutational burden scores were highest in the high *EIF4EBP1*-expression groups (all P<0.001). High *EIF4EBP1* expression significantly correlated to worse overall survival in all three cohorts (hazard ratios (HR) 1.4-1.9), and worse distant relapse-free survival in patients treated with neoadjuvant taxane-anthracycline chemotherapy (HR 2.4). GSEA demonstrated enriched mTOR and cell proliferation-related gene sets, including, MYC, G2M checkpoint, and E2F targets across all three bulk tumor and single cell RNA sequencing cohorts. Phenotypically, these pathways were reflected by increased Ki67 gene expression and signaling via pharmacologically-activated mTOR gene sets in *EIF4EBP1* high-expressing tumors (all P<0.001). *EIF4EBP1* expression was increased in whole breast tumors compared to normal breast tissue (P<0.001), and was expressed predominantly in cancer epithelial cells, particularly in basal epithelial cell subclasses. *EIF4EBP1* expression did not correlate to a consistent immune system phenotype across all three cohorts. Overall, these findings support that high *EIF4EBP1* gene expression in bulk breast tumors could represent a poor prognostic marker via mTOR signaling pathways activation and upregulation of cell cycling, ultimately leading to increased tumorigenesis.

Keywords: Bioinformatics, cap-dependent translation, mutational burden, prognostic biomarker, tumor progression, tumor microenvironment

Introduction

With a 1 in 8 lifetime risk, breast cancer is the most common cancer in women, and though five-year survival approaches 99% when managed as a localized condition, 43,000 women still die annually in the United States from this disease [1-3]. The majority of these deaths are attributable to the evolution of treatment resistance in disease that relapses [4]. Decoding these mechanisms of resistance is a cornerstone of current breast cancer research [5].

One of these pathways implicated in treatment resistance is the phosphoinositide 3-kinase (PI3K)/AKT/mammalian target of rapamycin

(mTOR) pathway, which is a major intracellular system that activates multiple cellular proliferation and metabolism networks in cancer cell signaling [6, 7]. In luminal breast cancers, the PI3K pathway is one of the most altered signaling cascades [8], and is upregulated in over 70% of all breast cancers [9]. At any step within this pathway, either overexpression or mutations result in pathway hyperactivation, which funnels into mTOR complex-1 (MTORC1)-mediated phosphorylation and initiation of multiple downstream transcriptional activators [8]. Specific to breast cancer treatment resistance, PI3K pathway hyperactivation, typically via activating mutations in *PI3KCA*, the gene encoding the p1110 alpha subunit, will promote escape from hormone dependence in estrogen receptor (ER) positive breast cancer [10] and trastuzumab resistance in human epidermal growth factor (HER2) positive breast cancer [11], regardless of tumor stage [12, 13]. As such, the mTOR inhibitor everolimus was the first oral targeted therapy widely used in advanced hormone positive breast cancer [14, 15], and is additionally known to extend progression-free survival in patients with trastuzumab-resistant HER2-postive advanced breast cancer [16].

One of the many downstream targets of the PI3K/ATK/mTOR pathway is eukaryotic translation initiation factor (EIF) 4E binding protein 1 (4E-BP1), encoded by the gene *EIF4EBP1* (**Figure 1**) [17]. 4E-BP1, in its unphosphorylated state, functions as a translation suppressor by preventing the eukaryotic translation factor 4E from complexing with a multisubunit scaffold that recruits the 40S ribosomal subunit to the 5' end of mRNA to initiate cap-dependent translation (**Figure 1**) [18]. The mTORC1 complex, in response to PI3K pathway activation, is the major kinase responsible for phosphorylating 4E-BP1, resulting in release of 4E and subsequent activation of cap-dependent translation [19]. Therefore, unphosphorylated 4E-BP1 can, in principle, act as a tumor suppressor [20]. Clinically however, 4E-BP1 is overexpressed in many tumor types including breast cancer relative to normal and benign tissue, and phosphorylated 4E-BP1 levels positively correlate with increased tumor size, lymph node metastasis, and locoregional breast cancer recurrence [21]. However, as a prognostic biomarker, the clinical relevance of *EIF4EBP1* gene expression is poorly understood.

In this study, we investigate the role of *EIF4EBP1* gene expression within the human breast cancer tumor microenvironment using bioinformatical analyses of transcriptomic profiles, as previously published by our group [22-27]. We hypothesize that *EIF4EBP1* gene expression in breast cancer is correlated to increased mTOR-mediated signaling and poor prognosis secondary to increased tumor cell proliferation. By exploring bulk tumor transcriptomics with the aid of gene set enrichment analysis (GSEA) [28] and cell cybersorting with the xCell algorithm [29], we can perform concurrent examinations of multiple cellular markers, functions, and tumor microenvironment (TME) interactions. Combining this data with associated patient clinical outcomes over multiple independent databases validates our conclusions on the clinical significance of *EIF4EBP1* gene expression in breast cancer.

Methods

Data acquisition

The primary data in this study was acquired from three main databases: the Cancer Genome Atlas Program (TCGA, whole database n=1090, estrogen-receptor positive and human epidermal growth factor negative tumors (ER+HER2-) n=593, HER2+ n=184, and triple negative breast cancer (TNBC) n=160), the Molecular Taxonomy of Breast Cancer International Consortium (METABRIC) (whole database n=1904, ER+HER2- n=1355, HER2+ n=236, TNBC n=313), and Sweden Cancerome Analysis Network-Breast (SCAN-B, GSE96058) (whole database n=3069, ER+HER2- n=2277, HER2+ n=392, TNBC n=155). TCGA and METABRIC results were obtained via the cBioPortal (https://www.cbioportal.org), and the expression data for TCGA was log-transformed using "data_mrna_seq_v2_rsem", while the METABRIC data was used as is with the "data_expression_median". SCAN-B results were downloaded from the Gene Expression Omnibus (GEO) repository of the United States National Institutes of Health (https://www.ncbi.nlm.nih.gov/geo), as described, and the provided normalized expression data from the database was used without any further processing [23, 30]. Data was also obtained from GSE25066 via GEO, a cohort comprised of 508 patients treated with neoadjuvant taxane-

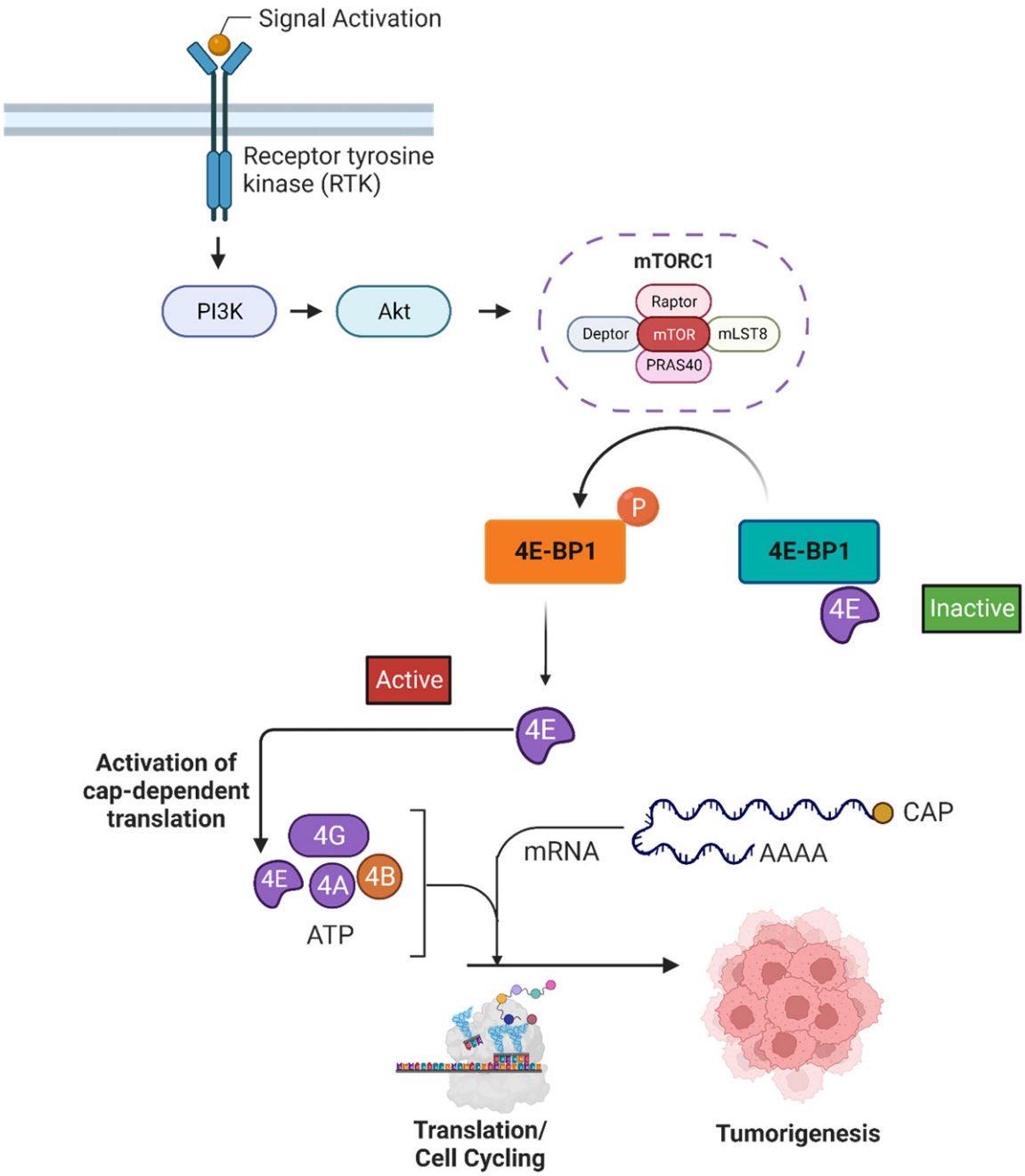

Figure 1. Overview of cellular signaling mediated by 4E-BP1 (4E binding protein 1). The 4E-BP1 protein is encoded by the gene *EIF4EBP1* (eukaryotic translation initiation factor 4EBP1). 4E-BP1 directly interacts with the eukaryotic translation factor 4E (4E), which prevents completion of a multisubunit scaffold that aids in the recruitment of 40S ribosomal subunits to the 5' end of mRNA. In response to mTOR (mammalian target of rapamycin) signaling following activation of the PI3K pathway (phosphoinositide 3-kinase)/AKT pathway, the mTORC1 complex will phosphorylate 4E-BP1. The enables the release of 4E, which is now free to complete the multisubunit scaffold necessary to activate cap-dependent translation of mRNA. Ultimately, this facilitates a broad range of downstream effects resulting in cell cycling and tumorigenesis.

anthracycline chemotherapy [31]. Gene expression data from 114 samples of normal breast tissue from female patients was obtained from the Genotype-Tissue Expression (GTex) Portal (https://gtexportal.org) [32].

Single cell RNA sequencing breast cancer atlas data from female patients was obtained from two large cohorts [33, 34] via the Broad Institute Single Cell Portal (https://singlecell.broadinstitute.org/single_cell), using the ac-

cession numbers SCP1039 [33] and SCP1106 [34]. The downloaded features, matrix, and barcode data were integrated and processed using the ReadMtx function in the Seurat package of R-4.2.1 (https://www.R-project.org), as previously described [25]. All R packages used in this project are previously described [25].

As 99.4 percent of all breast cancer cases occur in females [35], and all databases used in the study contain only female patients, male breast cancer was not examined in this study. All data was downloaded in July 2022. Because all data was obtained from deidentified public databases or cohorts, ethics approval requirements were waived by the Roswell Park Institutional Review Board.

Gene set enrichment analysis

Functional enrichment analysis of *EIF4EBP1* was performed by gene set enrichment analysis (GSEA) [28] on the Molecular Signatures Database Hallmark collection (http://www.gsea-msigdb.org) [36]. Gene sets with a false discovery rate (FDR) <0.25 specified enriched signaling [28]. High and low *EIF4EBP1* expression groups were dichotomized by median gene expression. Positive normalized enriched scores (NES) indicate enriched signaling in the *EIF4EBP1*-high expression group.

Other scores

The xCell algorithm (https://xcell.ucsf.edu) [29] was used to correlate *EIF4EBP1* expression to the infiltrating fraction of tumor and stromal cells (epithelial cells, fibroblasts, adipocytes, and endothelial cells), and immune cells (CD8+, T helper cell (Th)1 and Th2 cells, T-regulator cells, M1 and M2 macrophages, and dendritic cells) as described [22, 37-39]. The breast cancer mutational landscape (intratumor heterogeneity, homologous recombination defects, fraction genome altered, silent mutation rate, non-silent mutation rate, single-nucleotide neoantigens, and indel mutations) was examined from data derived by Thorsson *et al*. [40]. Immune cytolytic activity (CYT) in the tumor microenvironment was calculated as the geometric mean of the expression of perforin (*PRF1*) and granzyme A (*GZMA*) mRNA expression, which measures the anti-cancer ability of cytotoxic T cells [41].

Statistical analyses

Statistical analyses and figure production were performed with R-4.2.1 and BioRender (https://www.biorender.com). mRNA levels for *EIF4EBP1* were dichotomized into low and high groups based on the median expression level. All results are plotted as box plots, with the lower and upper bounds representing the maximum and minimum values, the upper and lower ends of box representing the 25th and 75th percentile values and the bolded bar within the box representing the median value. For TCGA results (RNA sequencing data), units of expression are log2 transformed RSEM, METABRIC (microarray data), units of expression are log intensity levels, and all GSE results (RNA sequencing data) are log2 transformed CPM. Two group comparisons were performed using the Mann-Whitney U test and multiple group comparisons by the Kruskal-Wallis test. The R survival software package was used to analyze survival based on high or low *EIF4EBP1* expression via Cox-proportional hazards regression, and Kaplan-Meier curves were compared by the log rank test. $P<0.05$ was set for statistical significance.

Results

Demographic data for patients in the three cohorts are presented in **Table 1**. Histograms of *EIF4EBP1* gene expression in each of TCGA, METABRIC, and SCAN-B show a relatively bell-shaped distribution with a slightly left-shifted curve (**Figure 2A**). In all three cohorts, *EIF4EBP1* expression was significantly highest in TNBCs and lowest in ER+HER2- tumors (all $P<0.001$, **Figure 2B**). There was a slight tendency for increased expression from stage I to stage III disease in the TCGA and METABRIC cohorts (staging data not available for SCAN-B) (**Figure 2C**). Tumors with positive lymph nodes had the same expression levels as node negative tumors (not shown). There was no difference between metastatic and non-metastatic tumors, however, there were only 29 metastatic tumors (stage IV) in TCGA and METABRIC combined (not shown). *EIF4EBP1* expression positively correlated with increasing tumor grade in all three cohorts (all $P<0.001$, **Figure 2D**).

Because tumor mutational burden is typically a molecular surrogate biomarker of disease aggressiveness [42], we examined a panel of

Table 1. Demographic data of patients in the three cohorts

Cohort	TCGA			METABRIC			SCAN-B		
Group	High	Low	*p*-value	High	Low	*p*-value	High	Low	*p*-value
Median Age (max, min)	58 (49, 69)	58 (48, 66)	0.3	61 (51, 70)	62 (52, 71)	0.14	65 (52, 73)	64 (53, 70)	0.08
Stage, N (%)			0.3			<0.001			N/A
I	79 (15%)	99 (18%)		193 (20%)	282 (30%)				
II	312 (58%)	298 (55%)		427 (45%)	373 (39%)				
III	122 (22%)	123 (23%)		75 (8%)	40 (4%)				
Unknown	26 (5%)	18 (3%)		257 (27%)	257 (27%)		1,535 (100%)	1,534 (100%)	
Lymph Node Involvement, N (%)			0.7			0.049			0.023
Negative	255 (47%)	253 (47%)		475 (50%)	518 (54%)		875 (57%)	936 (61%)	
Positive	269 (50%)	279 (52%)		477 (50%)	434 (46%)		611 (40%)	551 (36%)	
Unknown	15 (3%)	6 (1%)		0 (0%)	0 (0%)		49 (3%)	47 (3%)	
Subtype, N (%)			<0.001			<0.001			<0.001
ER+HER2-	231 (43%)	353 (66%)		555 (58%)	800 (84%)		995 (65%)	1,282 (84%)	
HER2+	92 (17%)	89 (17%)		148 (16%)	88 (9%)		250 (16%)	142 (9%)	
TNBC	130 (24%)	29 (5%)		249 (26%)	64 (7%)		134 (9%)	21 (1%)	
Unknown	86 (16%)	67 (12%)		0 (0%)	0 (0%)		156 (10%)	89 (6%)	
Grade, N (%)			<0.001			<0.001			<0.001
1	23 (4%)	53 (10%)		44 (5%)	121 (13%)		124 (8%)	330 (22%)	
2	96 (18%)	170 (32%)		288 (30%)	452 (47%)		571 (37%)	868 (57%)	
3	161 (30%)	73 (14%)		588 (62%)	339 (36%)		803 (52%)	312 (20%)	
Unknown	259 (40%)	242 (45%)		32 (3%)	40 (4%)		37 (2%)	24 (2%)	

High and low groupings are divided by median *EIF4EBP1* gene expression.

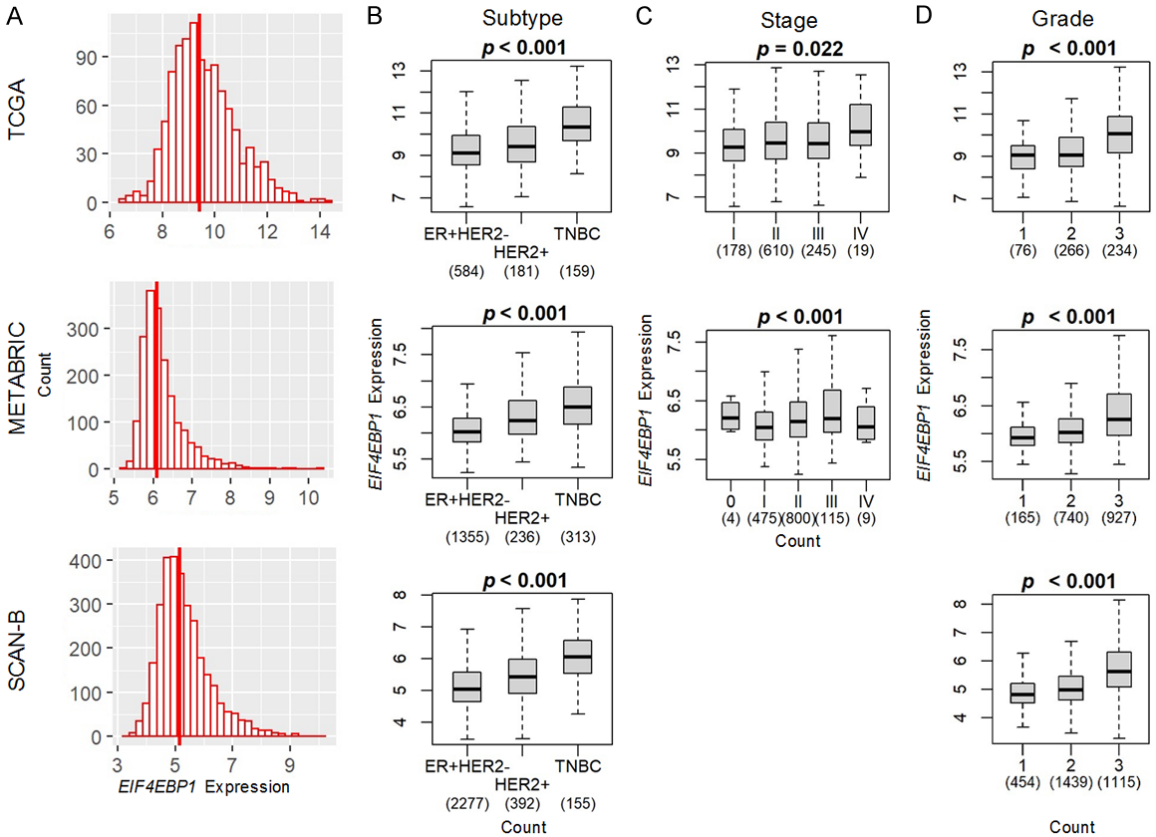

Figure 2. *EIF4EBP1* gene expression by breast cancer characteristics. A. Histogram distribution of *EIF4EBP1* expression in breast tumors in TCGA (1090 specimens), METABRIC (1094 specimens), and SCAN-B (3069 specimens). B. Breast cancer subtype. ER+HER2- (estrogen receptor positive, human epidermal growth factor receptor negative

tumors), HER2+, TNBC (triple negative breast cancer). C. Staging according to the American Joint Committee on Cancer (AJCC). Stage is not available for the SCAN-B cohort. D. Grading indicated according to AJCC. Counts for boxplots are indicated in the x-axis. Units of *EIF4EBP1* expression: TCGA - log2 transformed RSEM, METABRIC - log intensity levels, and SCAN-B - log2 transformed CPM. The bolded center bar within the box plots represents the median, the lower and upper box bounds represent the 25th and 75th percentiles, respectively, and the lower and upper tails represent the minimum and maximum values, respectively.

common mutational burden scores dichotomized by median *EIF4EBP1* expression. All scores (intratumor heterogeneity, homologous recombination defects (HRDs), fraction-genome-altered (FGR), silent mutation rate (SMR), non-silent mutation rate (NSMR), single-nucleotide variant (SNV) neoantigens, and indel mutations) were significantly elevated in the *EIF4EBP1*-high expressing group (all $P<0.001$, **Figure 3**).

We next examined survival trends dichotomized by the median into low and high *EIF4EBP1* expression. When comparing disease-free survival (DFS), the hazard ratio was about 1.3-1.4 for the high *EIF4EBP1* group compared to the low group in both TCGA and METABRIC. However, this result did not reach statistical significance in the TCGA group (HR 1.39, 95% confidence interval (CI) 0.96-2.04, P=0.08), but with nearly double the number of patients in METABRIC, the HR was 1.30 (1.12-1.52) (P=0.0007, **Figure 4A**). Disease-specific survival (DSS) was significant in both cohorts, with HR 1.4-1.8 (**Figure 4A**). Overall survival (OS) was a reported metric in all three large cohorts, and the HR was significant in all cohorts, with a HR of mortality ranging from 1.2-1.9 when comparing the high *EIF4EBP1* group to the low group (all P≤0.04, **Figure 4A**, **4B**). We additionally examined distant relapse-free survival (DRFS) for the GSE25066 cohort, which is comprised of 508 patients treated with neoadjuvant taxane-anthracycline chemotherapy [31]. The HR for DRFS was 2.38 (1.61-3.57) when comparing the high *EIF4EBP1* group to the low group (**Figure 4C**).

We used GSEA on the Hallmark pathways to correlate enriched gene signaling to *EIF4EBP1* expression [36]. Gene sets were selected if they were significantly enriched in all three cohorts. Of the 50 gene sets, 8 were enriched, and all of them were enriched in the high *EIF4EBP1* expression group. These included MTORC1 signaling, four cell-cycle related pathways (MYC Targets V1 and V2, G2M checkpoint, and E2F targets), unfolded protein response, glycolysis, and DNA repair, with all normalized enrichment scores (NES) in the 1.4-2.2 range (**Figure 5A**). We then repeated the GSEA analysis on two independent cohorts of single cell RNA sequenced tumors [33, 34]. In both cohorts, gene pathways for MTORC1 signaling, MYC targets V1, E2F targets, G2M checkpoint, and mitotic spindle occupied five of the top six highest NES gene sets (**Figure 5B**). We then examined whether pathway enrichment in cell cycling and MTORC1 signaling networks correlated to functional tumor biology. In all three cohorts, gene expression of Ki67, a marker of cell proliferation, was significantly increased in the high *EIF4EBP1* expression group compared to the lower expression group, consistent with cell cycling pathway gene enrichment (all P<0.001, **Figure 5C**). Similarly, we examined two gene signatures defined pharmacologically by gene upregulation following mTOR inhibition [43, 44]. These gene signatures were also significantly upregulated in the high *EIF4EBP1* expression group in all three cohorts (all P< 0.001, **Figure 5D**). We also examined the converse, by correlating a gene signature defined pharmacologically by gene downregulation following mTOR inhibition [43]. As predicted, this gene signature was significantly downregulated in the high *EIF4EBP1* expression group (all P<0.001, **Figure 5D**).

EIF4EBP1 expression levels were compared between normal breast tissues and whole breast tumors, and was significantly increased in the breast tumor group in TCGA (P<0.001, **Figure 6A**). We then used the xCell algorithm to examine tumor cell population estimates based on dichotomized *EIF4EBP1* expression. Epithelial cells were significantly increased in the high *EIF4EBP1* group in both TCGA and METABRIC cohorts (P<0.001), but was unchanged in the SCAN-B cohort (P=0.08, **Figure 6B**). Fibroblasts, adipocytes, and endothelial cell populations were decreased in the high

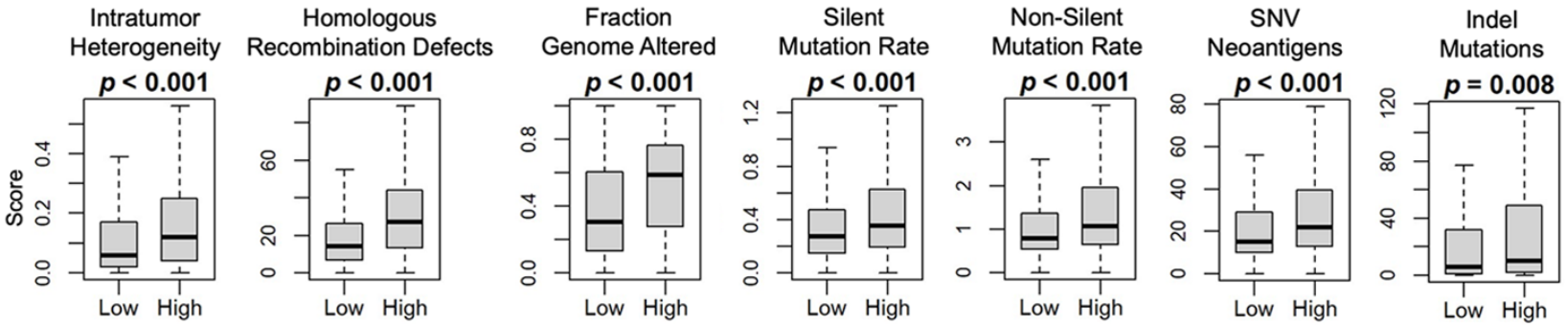

Figure 3. *EIF4EBP1* gene expression association with breast cancer mutations. Box plots of intratumor heterogeneity, homologous recombination defects, fraction genome altered, silent mutation rate, non-silent mutation rate, single-nucleotide variant (SNV) neoantigens, and indel mutations. Data are based on the scores by Thorsson, *et al.* [40]. *EIF4EBP1* expression is dichotomized by median expression. The bolded center bar within the boxplots represents the median, the lower and upper box bounds represent the 25th and 75th percentiles, respectively, and the lower and upper tails represent the minimum and maximum values, respectively.

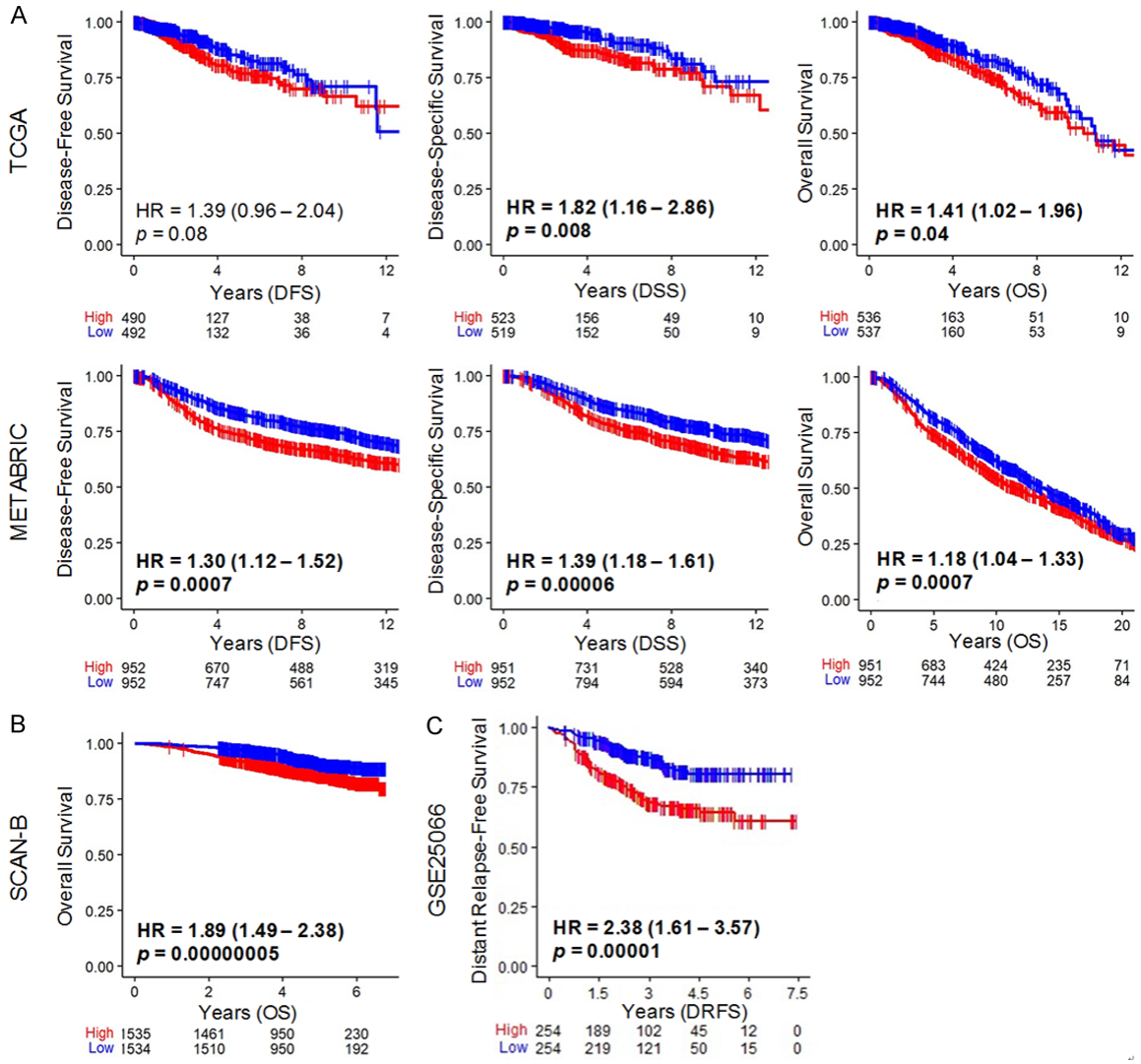

Figure 4. Survival plots for low and high *EIF4EBP1* gene expression in breast tumors. A. Disease-free survival (DFS), disease-specific survival (DSS), and overall survival (OS) for the TCGA and METABRIC cohorts. B. OS for the SCAN-B cohort. C. Distant relapse-free survival (DRFS) for the GSE25066 cohort. This cohort is comprised of 508 patients treated with neoadjuvant taxane-anthracycline chemotherapy [31]. Patients at risk for each time point are listed along the x-axis. *EIF4EBP1* expression is dichotomized into low and high groups by the median. The hazard ratio (HR) compares the high group against the low group. *P* values by log rank test.

EIF4EBP1 groups (**Figure 6B**). On analysis of two independent cohorts of single cell RNA sequencing results [33, 34], the bulk of *EIF-4EBP1* expression was attributable to epithelial/cancer epithelial cell populations (**Figure 6C**). When examined by epithelial cell subclass, the highest *EIF4EBP1* expression was found in basal epithelial cells rather than luminal (mature) epithelial cells (**Figure 6D**). We then finally examined the correlation between immune cell populations and *EIF4EBP1* expression levels. Among anti-cancer immune cells, Th1 cells and M1 macrophages were significantly increased in the high *EIF4EBP1* expression group in all three cohorts (all P<0.001), but there were no consistent trends for CD8+ T-cells or dendritic cells (**Figure 7**). Among pro-cancer immune cells, Th2 were significantly increased in the high *EIF4EBP1* expression group in all three cohorts (all P<0.001), but there were no consistent trends in regulatory T cells or M2 macrophages (**Figure 7**). As a surrogate measure of overall tumor immune response in the TME, immune cytolytic activity

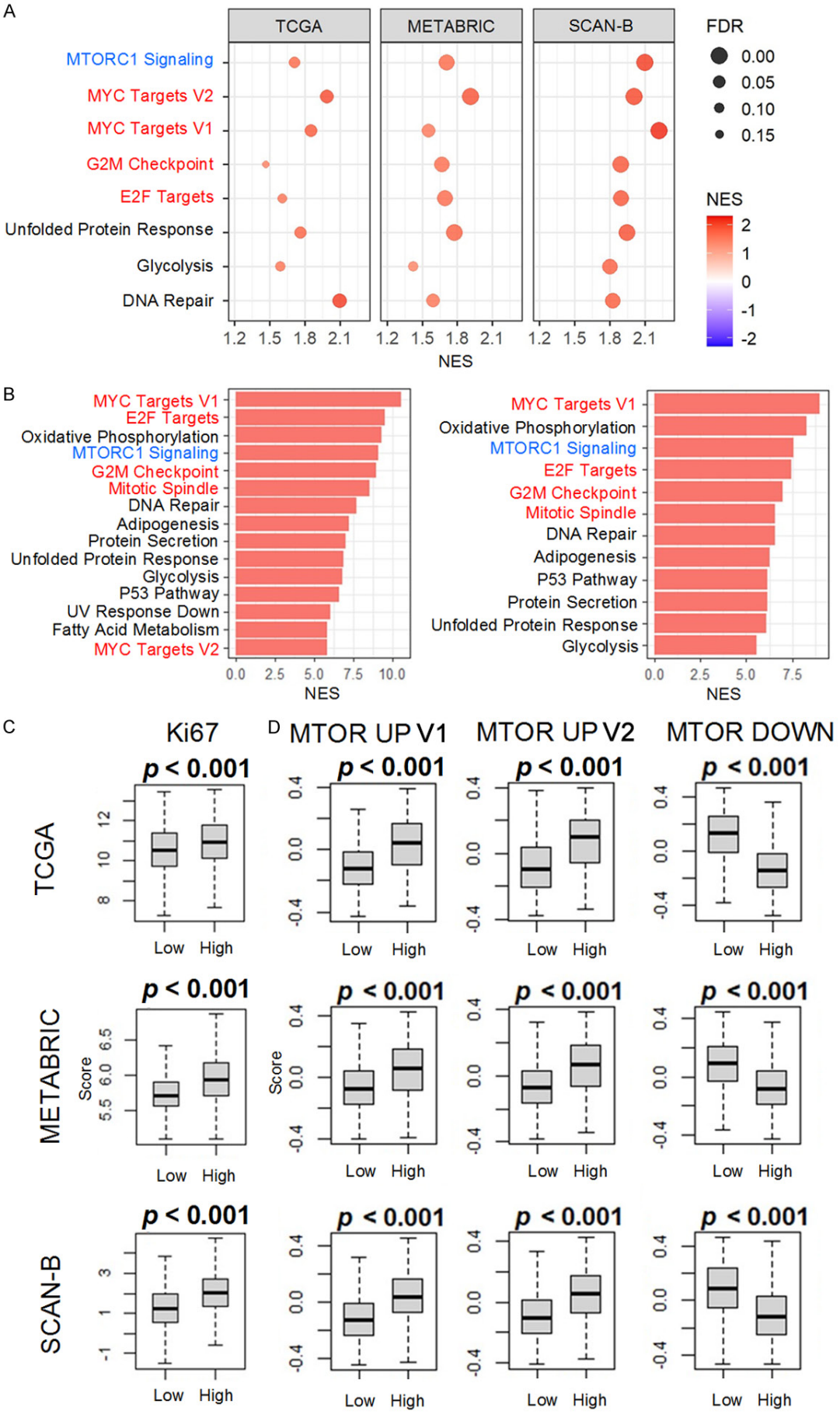
A
TCGA
METABRIC
SCAN-B
MTORC1 Signaling
MYC Targets V2
MYC Targets V1
G2M Checkpoint
E2F Targets
Unfolded Protein Response
Glycolysis
DNA Repair
1.2 1.5 1.8 2.1
NES
FDR
0.00
0.05
0.10
0.15
NES
2
1
0
-1
-2
B
MYC Targets V1
E2F Targets
Oxidative Phosphorylation
MTORC1 Signaling
G2M Checkpoint
Mitotic Spindle
DNA Repair
Adipogenesis
Protein Secretion
Unfolded Protein Response
Glycolysis
P53 Pathway
UV Response Down
Fatty Acid Metabolism
MYC Targets V2
0.0 2.5 5.0 7.5 10.0
NES
MYC Targets V1
Oxidative Phosphorylation
MTORC1 Signaling
E2F Targets
G2M Checkpoint
Mitotic Spindle
DNA Repair
Adipogenesis
P53 Pathway
Protein Secretion
Unfolded Protein Response
Glycolysis
0.0 2.5 5.0 7.5
NES
C
Ki67
D
MTOR UP V1
MTOR UP V2
MTOR DOWN
TCGA
METABRIC
SCAN-B
p < 0.001
Score
Low
High

Figure 5. Gene set enrichment analysis (GSEA) for *EIF4EBP1* in breast cancer, and demonstration of increased Ki67 and mTOR signaling in high expressing *EIF4EBP1*-tumors. (A) GSEA results from the Hallmark gene sets significant in all three cohorts (TCGA, METABRIC, and SCAN-B). A false discovery rate (FDR) of less than 0.25 was considered statistically significant. Dot size represents the FDR value, and they are colored according to the normalized enrichment score (NES). MTORC1 signaling gene set labelled in blue, and cell cycling-related gene sets labelled in red. (B) Most enriched gene sets in single cell RNA sequencing cohorts from cohorts described in [33] (left), and in [34] (right). MTORC1 signaling gene set labelled in blue, and cell cycling-related gene sets labelled in red. (C) Ki67 box plots based on median *EIF4EBP1* expression. (D) MTOR gene set defined by genes upregulated following siroliumus treatment as described in [43] (Left). MTOR gene set defined by genes upregulated following everolimus treatment as described in [44] (Middle). MTOR gene set defined by genes downregulated following siroliumus treatment as described in [43] (Right). For results in (C) and (D), *EIF4EBP1* expression is dichotomized into low and high groups by the median. The bolded center bar within the boxplots represents the median, the lower and upper box bounds represent the 25th and 75th percentiles, respectively, and the lower and upper tails represent the minimum and maximum values, respectively.

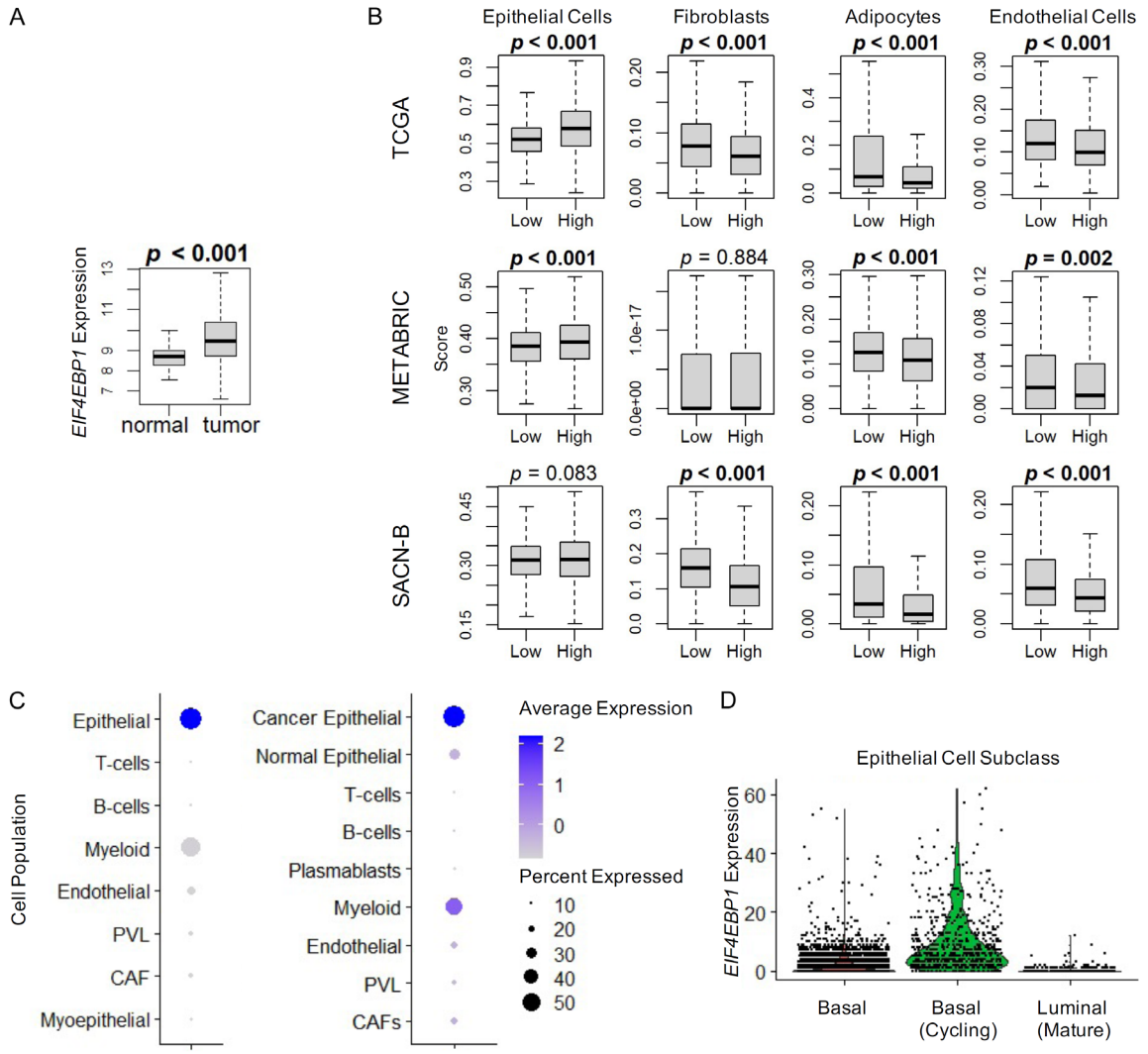

Figure 6. *EIF4EBP1* gene expression is enriched in breast tumors compared to normal breast tissues and is expressed primarily in cancer epithelial cells. A. mRNA expression from 114 normal breast tissues is compared to 1090 breast cancer tumors from the TCGA database. B. Box plots of epithelial cells, fibroblasts, adipocytes, and endothelial cells based on the xCell algorithm for the TCGA, METABRIC, and SCAN-B cohorts. *EIF4EBP1* gene expression is dichotomized by the median. The bolded center bar within the boxplots represents the median, the lower and upper box bounds represent the 25th and 75th percentiles, respectively, and the lower and upper tails represent the minimum and maximum values, respectively. C. Single cell RNA sequencing results from cohort described in [33],

comprised of 26 tumors (11 ER+HER2-, 5 HER2+, and 10 TNBC), with a total of 130,246 single cells (Left). Results from cohort described in [34] comprised of 5 TNBC tumors, with a total of 24,271 single cells (Right). D. The dot plot shows the overall percentage of the total *EIF4EBP1* gene expression by cell type and the average expression within each cell type for each cohort. Histogram/violin plot of *EIF4EBP1* gene expression by epithelial cell subclass from cohort described in [33].

(CYT score) showed no consistent pattern across the three cohorts (**Figure 7**).

Discussion

In this investigation, high expression of *EIF-4EBP1* was identified as a predictor for worsened breast cancer prognosis and validated in three independent cohorts with over 5000 patients. Breast cancers express increased *EIF4EBP1* levels compared to normal tissue. *EIF4EBP1* expression occurred primarily in cancer epithelial cells, and high *EIF4EBP1* expression correlated with increased tumor grade, increased overall tumor mutational burden, and decreased patient survival metrics. In these high expressing tumors, mTOR signaling and subsequent cell-cycle pathways were the most upregulated gene signatures. These gene signature findings were further supported by increased expression of gene sets characterized by mTOR pharmacological inhibition, and increased Ki67 scores.

EIF4EBP1 amplification has been demonstrated to occur across all breast cancer subtypes in up to 14% of cases [45]. While this might partially account for increased levels in breast tumors over normal tissue, it does not directly explain why high *EIF4EBP1* level correlate with increased tumorigenesis. As previously described, as protein, 4E-BP1 exists essentially in two states: unphosphorylated and phosphorylated. In the unphosphorylated state, 4E-BP1 functions as a both a transcriptional regulator and potential tumor suppressor by blocking cap-dependent translation via sequestration of the 4E transcription factor [20]. Particularly in response to mTOR-mediated signaling, 4E-BP1 becomes phosphorylated, releasing 4E for subsequent function [21]. In multiple cancer sites, including adrenocortical carcinoma, bladder urothelial, breast, ovarian, endometrial, renal, lung, mesothelioma, hepatocellular and acute myeloid leukemia, phosphorylated 4E-BP1 correlates to poor patient outcomes [45-48]. However, notability for gastric adenocarcinomas, phosphorylated 4E-BP1 is known to be highly expressed in early rather than late stage cancers, and is correlated with both prolonged disease-free and overall survival [48, 49].

Though not understood, there are several possible explanations for these discrepant findings among tumor sites. First, 4E-BP1 has at least seven sites of phosphorylation, each of which is likely to have their own influences on protein function regulation [17]. Second, these sites can be targeted by other minor kinases besides mTOR, including GSK-3 beta, ERK, PIM2, ATM, CDK1, and LRKK2, providing an additional level of modulation [17]. Third, there is evidence of spatial regulation of phosphorylated 4E-BP1 function. For example, cytoplasmic phosphorylated 4E-BP1 was observed in invasive breast and ovarian carcinomas as opposed to nuclear localization in normal epithelium and stromal tissues of the same tissue types [21]. However, in other tissue types, particularly endometrial cancer, nuclear rather than cytoplasmic phosphorylated 4E-BP1, correlated to both increased mTOR pathway activation and worse patient outcomes [50]. In summary, the proteomic, kinomic, and cellular localization aspects of 4E-BP1 regulation are extremely complex.

From this investigation, bulk tumor *EIF4EBP1* expression could be a much more straightforward surrogate marker for studying 4E-BP1 tumor biology in future breast cancer studies, as the tumorigenic phenotype exhibited in patients with elevated gene expression levels correlated strongly to known phosphorylated 4E-BP1-mediated characteristics. Mechanistically, this could be explained by the high likelihood that most 4E-BP1 in breast tumors exists in a phosphorylated state due secondary to nearly constitutive PI3K/mTOR pathway activity secondary to activating mutations [51]. Immunohistochemical investigations have showed expression levels of phosphorylated 4E-BP1 in breast tumors to be as high as 87% [21], or as low as 30% [52]. Such variability in part depends on the qualitative nature and even interpersonal variability of immunohistochemistry scoring [53]. To the best of our knowledge,

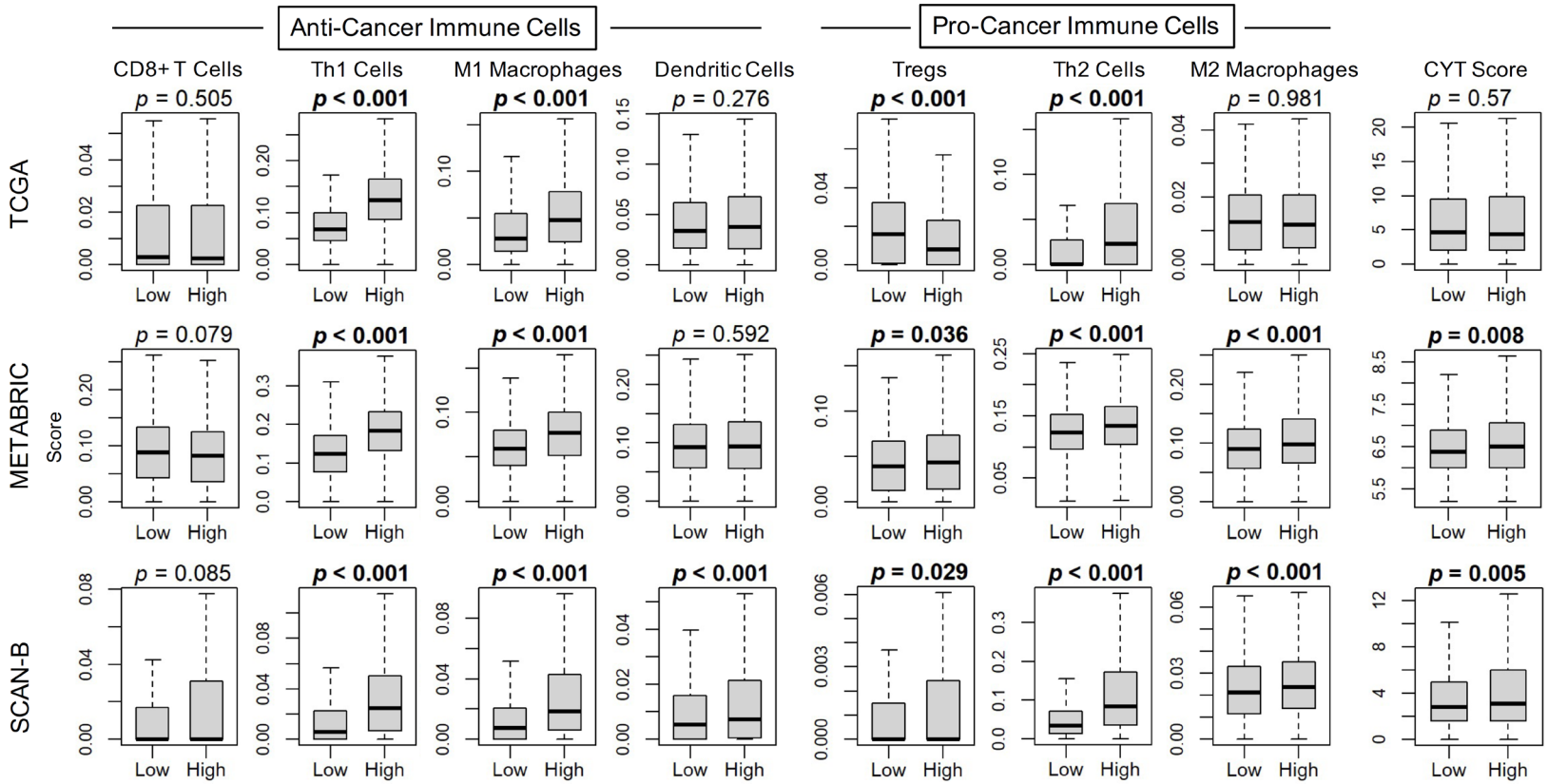

Figure 7. Anti-cancerous and pro-cancerous immune cell correlation with *EIF4EBP1* expression in breast cancer tumors, and cytolytic (CYT) scores. Box plots are based on the xCell algorithm for the TCGA, METABRIC, and SCAN-B cohorts. *EIF4EBP1* expression is dichotomized into low and high groups by the median. The bolded center bar within the boxplots represents the median, the lower and upper box bounds represent the 25th and 75th percentiles, respectively, and the lower and upper tails represent the minimum and maximum values, respectively.

there are no studies that have conducted patient-matched correlations of 4E-BP1 mRNA and phosphorylated protein levels.

While this study supports the clinical relevance of *EIF4EBP1* expression in breast cancer, it does have several limitations. Despite using three very large and widely used independent cohorts to validate our key findings, our study is retrospective in its design, and is therefore prone to selection bias. The absence of granular clinical information requires us to assume that all patients received standard of care treatments; these however are constantly in flux, and therefore patient populations, treatments, and outcomes are heterogeneous. Additionally, although we cannot necessarily deduce mechanism of action from bioinformatic data, these investigations offer powerful insights into the association between *EIF4EBP1* expression and patient outcomes, and are conducive to our proteomic understandings of signaling mediated by the pathways this binding protein modulates. Further comparative studies to systematically delineate the mechanistic underpinnings of the genomic, epigenic, proteomic, and kinomic pathways of the PI3K/mTOR/4E-BP1 network would provide invaluable information to tailor and further design clinical trials for novel adjuvant therapeutics to mitigate breast cancer therapy resistance.

Acknowledgements

This research was supported by the National Institutes of Health, USA grant numbers R37CA248018, R01CA250412, R01CA251545, R01EB029596, the US Department of Defense BCRP grant numbers W81XWH-19-1-0674 and W81XWH-19-1-0111 to K.T., and the National Cancer Institute Cancer Center Support Grant P30CA016056 to Roswell Park Comprehensive Cancer Center.

Disclosure of conflict of interest

None.

Address correspondence to: Dr. Kazuaki Takabe, Department of Surgical Oncology, Roswell Park Comprehensive Cancer Center, Elm and Carlton Streets, Buffalo, NY 14263, USA. Tel: 1-716-845-5540; E-mail: kazuaki.takabe@roswellpark.org

References

[1] Siegel RL, Miller KD, Fuchs HE and Jemal A. Cancer statistics, 2022. CA Cancer J Clin 2022; 72: 7-33.

[2] Wang R, Zhu Y, Liu X, Liao X, He J and Niu L. The clinicopathological features and survival outcomes of patients with different metastatic sites in stage IV breast cancer. BMC Cancer 2019; 19: 1091.

[3] Centers for Disease Control and Prevention. U.S. cancer statistics female breast cancer stat bite. US Department of Health and Human Services 2022.

[4] Benesch MGK, Tang X and Brindley DN. Autotaxin and breast cancer: towards overcoming treatment barriers and sequelae. Cancers (Basel) 2020; 12: 374.

[5] Lainetti PF, Leis-Filho AF, Laufer-Amorim R, Battazza A and Fonseca-Alves CE. Mechanisms of resistance to chemotherapy in breast cancer and possible targets in drug delivery systems. Pharmaceutics 2020; 12: 1193.

[6] Paplomata E and O'Regan R. The PI3K/AKT/mTOR pathway in breast cancer: targets, trials and biomarkers. Ther Adv Med Oncol 2014; 6: 154-166.

[7] Ciuffreda L, Di Sanza C, Incani UC and Milella M. The mTOR pathway: a new target in cancer therapy. Curr Cancer Drug Targets 2010; 10: 484-495.

[8] Miricescu D, Totan A, Stanescu-Spinu II, Badoiu SC, Stefani C and Greabu M. PI3K/AKT/mTOR signaling pathway in breast cancer: from molecular landscape to clinical aspects. Int J Mol Sci 2020; 22: 173.

[9] Forbes SA, Bindal N, Bamford S, Cole C, Kok CY, Beare D, Jia M, Shepherd R, Leung K, Menzies A, Teague JW, Campbell PJ, Stratton MR and Futreal PA. COSMIC: mining complete cancer genomes in the catalogue of somatic mutations in cancer. Nucleic Acids Res 2011; 39: D945-950.

[10] Miller TW, Hennessy BT, González-Angulo AM, Fox EM, Mills GB, Chen H, Higham C, García-Echeverría C, Shyr Y and Arteaga CL. Hyperactivation of phosphatidylinositol-3 kinase promotes escape from hormone dependence in estrogen receptor-positive human breast cancer. J Clin Invest 2010; 120: 2406-2413.

[11] Fujimoto Y, Morita TY, Ohashi A, Haeno H, Hakozaki Y, Fujii M, Kashima Y, Kobayashi SS and Mukohara T. Combination treatment with a PI3K/Akt/mTOR pathway inhibitor overcomes resistance to anti-HER2 therapy in PIK3CA-mutant HER2-positive breast cancer cells. Sci Rep 2020; 10: 21762.

[12] Jensen JD, Knoop A, Laenkholm AV, Grauslund M, Jensen MB, Santoni-Rugiu E, Andersson M

and Ewertz M. PIK3CA mutations, PTEN, and pHER2 expression and impact on outcome in HER2-positive early-stage breast cancer patients treated with adjuvant chemotherapy and trastuzumab. Ann Oncol 2012; 23: 2034-2042.

[13] Baselga J, Cortés J, Im SA, Clark E, Ross G, Kiermaier A and Swain SM. Biomarker analyses in CLEOPATRA: a phase III, placebo-controlled study of pertuzumab in human epidermal growth factor receptor 2-positive, first-line metastatic breast cancer. J Clin Oncol 2014; 32: 3753-3761.

[14] François-Martin H, Lardy-Cléaud A, Pistilli B, Levy C, Diéras V, Frenel JS, Guiu S, Mouret-Reynier MA, Mailliez A, Eymard JC, Petit T, Ung M, Desmoulins I, Augereau P, Bachelot T, Uwer L, Debled M, Ferrero JM, Clatot F, Goncalves A, Chevrot M, Chabaud S and Cottu P. Long-term results with everolimus in advanced hormone receptor positive breast cancer in a multicenter national real-world observational study. Cancers (Basel) 2023; 15: 1191.

[15] Royce M, Bachelot T, Villanueva C, Özgüroğlu M, Azevedo SJ, Cruz FM, Debled M, Hegg R, Toyama T, Falkson C, Jeong J, Srimuninnimit V, Gradishar WJ, Arce C, Ridolfi A, Lin C and Cardoso F. Everolimus plus endocrine therapy for postmenopausal women with estrogen receptor-positive, human epidermal growth factor receptor 2-negative advanced breast cancer: a clinical trial. JAMA Oncol 2018; 4: 977-984.

[16] André F, O'Regan R, Ozguroglu M, Toi M, Xu B, Jerusalem G, Masuda N, Wilks S, Arena F, Isaacs C, Yap YS, Papai Z, Lang I, Armstrong A, Lerzo G, White M, Shen K, Litton J, Chen D, Zhang Y, Ali S, Taran T and Gianni L. Everolimus for women with trastuzumab-resistant, HER2-positive, advanced breast cancer (BOLERO-3): a randomised, double-blind, placebo-controlled phase 3 trial. Lancet Oncol 2014; 15: 580-591.

[17] Qin X, Jiang B and Zhang Y. 4E-BP1, a multifactor regulated multifunctional protein. Cell Cycle 2016; 15: 781-786.

[18] Richter JD and Sonenberg N. Regulation of cap-dependent translation by eIF4E inhibitory proteins. Nature 2005; 433: 477-480.

[19] Böhm R, Imseng S, Jakob RP, Hall MN, Maier T and Hiller S. The dynamic mechanism of 4E-BP1 recognition and phosphorylation by mTORC1. Mol Cell 2021; 81: 2403-2416, e2405.

[20] Armengol G, Rojo F, Castellví J, Iglesias C, Cuatrecasas M, Pons B, Baselga J and Ramón y Cajal S. 4E-binding protein 1: a key molecular "funnel factor" in human cancer with clinical implications. Cancer Res 2007; 67: 7551-7555.

[21] Rojo F, Najera L, Lirola J, Jiménez J, Guzmán M, Sabadell MD, Baselga J and Ramon y Cajal S. 4E-binding protein 1, a cell signaling hallmark in breast cancer that correlates with pathologic grade and prognosis. Clin Cancer Res 2007; 13: 81-89.

[22] Oshi M, Asaoka M, Tokumaru Y, Angarita FA, Yan L, Matsuyama R, Zsiros E, Ishikawa T, Endo I and Takabe K. Abundance of regulatory T cell (Treg) as a predictive biomarker for neoadjuvant chemotherapy in triple-negative breast cancer. Cancers (Basel) 2020; 12: 3038.

[23] Oshi M, Tokumaru Y, Benesch MG, Sugito N, Wu R, Yan L, Yamada A, Chishima T, Ishikawa T, Endo I and Takabe K. High miR-99b expression is associated with cell proliferation and worse patient outcomes in breast cancer. Am J Cancer Res 2022; 12: 4840-4852.

[24] Wu R, Oshi M, Asaoka M, Yan L, Benesch MGK, Khoury T, Nagahashi M, Miyoshi Y, Endo I, Ishikawa T and Takabe K. Intratumoral tumor infiltrating lymphocytes (TILs) are associated with cell proliferation and better survival but not always with chemotherapy response in breast cancer. Ann Surg 2023; 278: 587-597.

[25] Benesch MG, Wu R, Tang X, Brindley DN, Ishikawa T and Takabe K. Autotaxin production in the human breast cancer tumor microenvironment mitigates tumor progression in early breast cancers. Am J Cancer Res 2023; 13: 2790-2813.

[26] Okano M, Oshi M, Butash AL, Asaoka M, Katsuta E, Peng X, Qi Q, Yan L and Takabe K. Estrogen receptor positive breast cancer with high expression of androgen receptor has less cytolytic activity and worse response to neoadjuvant chemotherapy but better survival. Int J Mol Sci 2019; 20: 2655.

[27] Oshi M, Newman S, Tokumaru Y, Yan L, Matsuyama R, Kalinski P, Endo I and Takabe K. Plasmacytoid dendritic cell (pDC) infiltration correlate with tumor infiltrating lymphocytes, cancer immunity, and better survival in triple negative breast cancer (TNBC) more strongly than conventional dendritic cell (cDC). Cancers (Basel) 2020; 12: 3342.

[28] Subramanian A, Tamayo P, Mootha VK, Mukherjee S, Ebert BL, Gillette MA, Paulovich A, Pomeroy SL, Golub TR, Lander ES and Mesirov JP. Gene set enrichment analysis: a knowledge-based approach for interpreting genome-wide expression profiles. Proc Natl Acad Sci U S A 2005; 102: 15545-15550.

[29] Aran D, Hu Z and Butte AJ. xCell: digitally portraying the tissue cellular heterogeneity landscape. Genome Biol 2017; 18: 220.

[30] Wu R, Yu I, Tokumaru Y, Asaoka M, Oshi M, Yan L, Okuda S, Ishikawa T and Takabe K. Elevated

bile acid metabolism and microbiome are associated with suppressed cell proliferation and better survival in breast cancer. Am J Cancer Res 2022; 12: 5271-5285.

[31] Hatzis C, Pusztai L, Valero V, Booser DJ, Esserman L, Lluch A, Vidaurre T, Holmes F, Souchon E, Wang H, Martin M, Cotrina J, Gomez H, Hubbard R, Chacón JI, Ferrer-Lozano J, Dyer R, Buxton M, Gong Y, Wu Y, Ibrahim N, Andreopoulou E, Ueno NT, Hunt K, Yang W, Nazario A, DeMichele A, O'Shaughnessy J, Hortobagyi GN and Symmans WF. A genomic predictor of response and survival following taxane-anthracycline chemotherapy for invasive breast cancer. JAMA 2011; 305: 1873-1881.

[32] GTEx Consortium. The genotype-tissue expression (GTEx) project. Nat Genet 2013; 45: 580-585.

[33] Wu SZ, Roden DL, Wang C, Holliday H, Harvey K, Cazet AS, Murphy KJ, Pereira B, Al-Eryani G, Bartonicek N, Hou R, Torpy JR, Junankar S, Chan CL, Lam CE, Hui MN, Gluch L, Beith J, Parker A, Robbins E, Segara D, Mak C, Cooper C, Warrier S, Forrest A, Powell J, O'Toole S, Cox TR, Timpson P, Lim E, Liu XS and Swarbrick A. Stromal cell diversity associated with immune evasion in human triple-negative breast cancer. EMBO J 2020; 39: e104063.

[34] Wu SZ, Al-Eryani G, Roden DL, Junankar S, Harvey K, Andersson A, Thennavan A, Wang C, Torpy JR, Bartonicek N, Wang T, Larsson L, Kaczorowski D, Weisenfeld NI, Uytingco CR, Chew JG, Bent ZW, Chan CL, Gnanasambandapillai V, Dutertre CA, Gluch L, Hui MN, Beith J, Parker A, Robbins E, Segara D, Cooper C, Mak C, Chan B, Warrier S, Ginhoux F, Millar E, Powell JE, Williams SR, Liu XS, O'Toole S, Lim E, Lundeberg J, Perou CM and Swarbrick A. A single-cell and spatially resolved atlas of human breast cancers. Nat Genet 2021; 53: 1334-1347.

[35] Benesch MGK and Mathieson A. Epidemiology of mucinous adenocarcinomas. Cancers (Basel) 2020; 12: 3193.

[36] Liberzon A, Birger C, Thorvaldsdóttir H, Ghandi M, Mesirov JP and Tamayo P. The molecular signatures database (MSigDB) hallmark gene set collection. Cell Syst 2015; 1: 417-425.

[37] Tokumaru Y, Oshi M, Murthy V, Tian W, Yan L, Angarita FA, Nagahashi M, Matsuhashi N, Futamura M, Yoshida K, Miyoshi Y and Takabe K. Low intratumoral genetic neutrophil-to-lymphocyte ratio (NLR) is associated with favorable tumor immune microenvironment and with survival in triple negative breast cancer (TNBC). Am J Cancer Res 2021; 11: 5743-5755.

[38] Chouliaras K, Oshi M, Asaoka M, Tokumaru Y, Khoury T, Endo I, Ishikawa T and Takabe K. Increased intratumor heterogeneity, angiogenesis and epithelial to mesenchymal transition pathways in metaplastic breast cancer. Am J Cancer Res 2021; 11: 4408-4420.

[39] Le L, Tokumaru Y, Oshi M, Asaoka M, Yan L, Endo I, Ishikawa T, Futamura M, Yoshida K and Takabe K. Th2 cell infiltrations predict neoadjuvant chemotherapy response of estrogen receptor-positive breast cancer. Gland Surg 2021; 10: 154-165.

[40] Thorsson V, Gibbs DL, Brown SD, Wolf D, Bortone DS, Ou Yang TH, Porta-Pardo E, Gao GF, Plaisier CL, Eddy JA, Ziv E, Culhane AC, Paull EO, Sivakumar IKA, Gentles AJ, Malhotra R, Farshidfar F, Colaprico A, Parker JS, Mose LE, Vo NS, Liu J, Liu Y, Rader J, Dhankani V, Reynolds SM, Bowlby R, Califano A, Cherniack AD, Anastassiou D, Bedognetti D, Mokrab Y, Newman AM, Rao A, Chen K, Krasnitz A, Hu H, Malta TM, Noushmehr H, Pedamallu CS, Bullman S, Ojesina AI, Lamb A, Zhou W, Shen H, Choueiri TK, Weinstein JN, Guinney J, Saltz J, Holt RA and Rabkin CS; Cancer Genome Atlas Research Network; Lazar AJ, Serody JS, Demicco EG, Disis ML, Vincent BG and Shmulevich I. The immune landscape of cancer. Immunity 2018; 48: 812-830, e814.

[41] Wakiyama H, Masuda T, Motomura Y, Hu Q, Tobo T, Eguchi H, Sakamoto K, Hirakawa M, Honda H and Mimori K. Cytolytic activity (CYT) score is a prognostic biomarker reflecting host immune status in hepatocellular carcinoma (HCC). Anticancer Res 2018; 38: 6631-6638.

[42] Fusco MJ, West HJ and Walko CM. Tumor mutation burden and cancer treatment. JAMA Oncol 2021; 7: 316.

[43] Wei G, Twomey D, Lamb J, Schlis K, Agarwal J, Stam RW, Opferman JT, Sallan SE, den Boer ML, Pieters R, Golub TR and Armstrong SA. Gene expression-based chemical genomics identifies rapamycin as a modulator of MCL1 and glucocorticoid resistance. Cancer Cell 2006; 10: 331-342.

[44] Majumder PK, Febbo PG, Bikoff R, Berger R, Xue Q, McMahon LM, Manola J, Brugarolas J, McDonnell TJ, Golub TR, Loda M, Lane HA and Sellers WR. mTOR inhibition reverses Akt-dependent prostate intraepithelial neoplasia through regulation of apoptotic and HIF-1-dependent pathways. Nat Med 2004; 10: 594-601.

[45] Rutkovsky AC, Yeh ES, Guest ST, Findlay VJ, Muise-Helmericks RC, Armeson K and Ethier SP. Eukaryotic initiation factor 4E-binding protein as an oncogene in breast cancer. BMC Cancer 2019; 19: 491.

[46] Tang Y, Luo J, Yang Y, Liu S, Zheng H, Zhan Y, Fan S and Wen Q. Overexpression of p-4EBP1 associates with p-eIF4E and predicts poor

prognosis for non-small cell lung cancer patients with resection. PLoS One 2022; 17: e0265465.

[47] Naito S, Ichiyanagi O, Ito H, Kabasawa T, Kanno H, Narisawa T, Fukuhara H, Yagi M, Kurota Y, Yamagishi A, Sakurai T, Nishida H, Kawazoe H, Yamanobe T, Kato T, Makhov P, Kolenko VM, Yamakawa M and Tsuchiya N. Expression of total and phospho 4EBP1 in metastatic and non-metastatic renal cell carcinoma. Oncol Lett 2019; 17: 3910-3918.

[48] Du K, Zou J, Liu C, Khan M, Xie T, Huang X, Zhang K, Yuan Y and Wang B. A multi-omics pan-cancer analysis of 4EBP1 in cancer prognosis and cancer-associated fibroblasts infiltration. Front Genet 2022; 13: 845751.

[49] Lee HW, Park MI, Kim MS, Kim SH, Roh MS, Kim K, Jung SB and Lee EH. Overexpression of phosphorylated 4E-binding protein 1 and its clinicopathological significances in gastric cancer. Pathol Res Pract 2015; 211: 298-302.

[50] Darb-Esfahani S, Faggad A, Noske A, Weichert W, Buckendahl AC, Müller B, Budczies J, Röske A, Dietel M and Denkert C. Phospho-mTOR and phospho-4EBP1 in endometrial adenocarcinoma: association with stage and grade in vivo and link with response to rapamycin treatment in vitro. J Cancer Res Clin Oncol 2009; 135: 933-941.

[51] du Rusquec P, Blonz C, Frenel JS and Campone M. Targeting the PI3K/Akt/mTOR pathway in estrogen-receptor positive HER2 negative advanced breast cancer. Ther Adv Med Oncol 2020; 12: 1758835920940939.

[52] Karlsson E, Pérez-Tenorio G, Amin R, Bostner J, Skoog L, Fornander T, Sgroi DC, Nordenskjöld B, Hallbeck AL and Stål O. The mTOR effectors 4EBP1 and S6K2 are frequently coexpressed, and associated with a poor prognosis and endocrine resistance in breast cancer: a retrospective study including patients from the randomised Stockholm tamoxifen trials. Breast Cancer Res 2013; 15: R96.

[53] Baez-Navarro X, van Bockstal MR, Nawawi D, Broeckx G, Colpaert C, Doebar SC, Hogenes MCH, Koop E, Lambein K, Peeters DJE, Sinke RHJA, Bastiaan van Brakel J, van der Starre-Gaal J, van der Vegt B, van de Vijver K, Vreuls CPH, Vreuls W, Westenend PJ and van Deurzen CHM. Interobserver variation in the assessment of immunohistochemistry expression levels in HER2-negative breast cancer: can we improve the identification of low levels of HER2 expression by adjusting the criteria? An international interobserver study. Mod Pathol 2023; 36: 100009.